
Co-Reinforcement Learning for Unified Multimodal Understanding and Generation

Jingjing Jiang^{1,2}, Chongjie Si², Jun Luo¹, Hanwang Zhang¹, Chao Ma²

¹Nanyang Technological University, ²Shanghai Jiao Tong University

{jingjing.jiang, junluo, hanwangzhang}@ntu.edu.sg

{chongjiesi, chaoma}@sjtu.edu.cn

Abstract

This paper presents a pioneering exploration of reinforcement learning (RL) via group relative policy optimization for unified multimodal large language models (ULMs), aimed at simultaneously reinforcing generation and understanding capabilities. Through systematic pilot studies, we uncover the significant potential of ULMs to enable the synergistic co-evolution of dual capabilities within a shared policy optimization framework. Building on this insight, we introduce **CoRL**, a co-reinforcement learning framework comprising a unified RL stage for joint optimization and a refined RL stage for task-specific enhancement. With the proposed CoRL, our resulting model, **ULM-R1**, achieves average improvements of **7%** on three text-to-image generation datasets and **23%** on nine multimodal understanding benchmarks. These results demonstrate the effectiveness of CoRL and highlight the substantial benefit of reinforcement learning in facilitating cross-task synergy and optimization for ULMs.

1 Introduction

As large foundation models (LFMs) continue to advance in general capabilities and breadth of knowledge, post-training [27, 67, 101] has emerged as a critical paradigm for further refining pretrained LFMs toward specialized applications, facilitating task adaptation and human-aligned behaviors. Recently, reinforcement learning (RL)-based approaches [47, 48, 55, 60, 64, 66, 88] have exhibited considerable promise due to their data efficiency and strong alignment abilities. A notable exemplar is DeepSeek-R1 [18], which demonstrates that RL with verifiable rewards and the group relative policy optimization (GRPO) algorithm constitutes a practical and stable strategy that sidesteps explicit preference modeling [70] and reward model learning [76]. This promising paradigm indicates *the significant potential of LFMs to acquire advanced capabilities and generalize effectively without dependence on large-scale, high-quality supervised data*.

In the multimodal AI research community, the prevailing implementation [8, 22, 37, 38, 49, 64, 93, 94] of the GRPO algorithm centers on crafting diverse rule-based reward mechanisms to incentivize long-chain reasoning capabilities of multimodal large language models (MLLMs). These initiatives primarily target multimodal understanding, with particular focus on visual and mathematical reasoning tasks. Conversely, its application to visual generation remains surprisingly limited, with only pioneering explorations [23, 72] suggesting its feasibility. More importantly, extending GRPO to unified MLLMs (ULMs) [7, 36, 81, 83] capable of concurrently performing visual understanding and generation tasks remains considerably under-explored. Intuitively, ULMs could significantly benefit from GRPO owing to their inherent advantages of *cross-task synergy and LLM sharing*, which enables ULMs to share reward signals across various tasks and effectively mitigate reward imbalance, particularly when GRPO operates by jointly ranking outputs within task-agnostic groups.

This paper aims to enhance the understanding and generation capabilities of ULMs without dependence on supervised data. We begin with pilot experiments to explore efficient reinforcement learning paradigms. Specifically, we systematically examine four rule-based training strategies: (i) separate RL for individual tasks, (ii) separate RL with weight merging, (iii) cycle RL alternating between tasks, and (iv) unified RL with joint optimization. Our explorations reveal two critical findings. *First*, direct task-specific RL fails to achieve the anticipated improvements, particularly in visual generation, and even impairs other abilities. *Second*, compared with alternative strategies, unified RL showcases comprehensive advantages across tasks. These results demonstrate the synergistic co-evolution of dual capabilities under a shared policy optimization paradigm.

In light of our preliminary findings, we propose **CoRL**, a co-evolutionary reinforcement learning framework designed to synergistically improve the understanding and generation capabilities of ULMs. CoRL follows a two-stage RL procedure: a unified RL stage for joint optimization of dual capabilities and a refined RL stage for task-specific enhancement. In the first stage, the policy ULM is optimized through a unified GRPO algorithm with diverse rewards on a carefully curated dataset spanning both understanding and generation tasks. To effectively guide policy optimization in visual generation, we introduce a *bidirectional cycle consistency reward* and a *text-image matching reward*, which together promote semantic consistency and faithfulness of synthesized images to their corresponding prompts. The designed rewards complement typical multimodal understanding rewards (*i.e.*, accuracy and format) within a unified group, enabling cross-task joint optimization. In the subsequent stage, we independently reinforce the policy’s understanding and generation capabilities using respective rewards and tailored datasets for task-specific refinement.

Applying the two-stage CoRL training to the baseline ULM Janus-Pro [7] yields **ULM-R1**, a unified model with reinforced capabilities in both understanding and generation. To comprehensively assess its performance, we conduct extensive comparisons against state-of-the-art unified MLLMs and dedicated models across three visual generation and nine multimodal understanding benchmarks. Notably, ULM-R1 achieves substantial gains over its baseline on complex mathematical and logical reasoning tasks, such as WeMath (+15.2) and LogicVista (+10.6). These results underscore the effectiveness of CoRL, providing compelling empirical evidence for the efficacy of RL in simultaneously advancing visual understanding and generation tasks.

We summarize our main contributions as follows:

- We establish that RL with verifiable rewards and GRPO constitutes a data-efficient paradigm for cross-task co-optimization and capability enhancement.
- We introduce a co-evolutionary reinforcement learning framework, CoRL, to synergistically enhance the dual capabilities of ULMs using a unified-then-refined RL paradigm.
- We demonstrate the effectiveness of CoRL and the advantage of ULM-R1 through extensive qualitative and quantitative experiments across diverse benchmarks.

2 Related Work

Unified Multimodal Understanding and Generation. Recent advancements [7, 36, 62, 65, 69, 75, 79–81, 83, 84, 100] have witnessed increasing attention to jointly model multimodal understanding and visual generation within a unified model. Pioneering attempts [11, 16] predominantly rely on continuous diffusion models, integrating external diffusion decoders for image synthesis. Inspired by autoregressive next-token prediction, a growing line of research [7, 28, 36, 43, 53, 65, 75, 78–81] encode visual inputs into discrete tokens and generate images in a *fully autoregressive* (F-AR) manner. Specifically, this approach employs a vector quantized (VQ) tokenizer [13, 86] to convert images into discrete tokens, analogous to text tokenization. To mitigate information loss in VQ discretization, another stream of work [15, 21, 26, 44, 69, 83, 85] explores *autoregressive and diffusion* (AR-Diff) hybrid modeling approaches. Architecturally, these models typically comprise a vision autoencoder, a text tokenizer, and an LLM. This work builds upon the F-AR model to develop an effective reinforcement learning framework.

RL-based Post-Training for MLLMs. Post-training [101] aims to further enhance the performance of pretrained models for customized applications and user needs. Recently, RL [71, 77] has emerged as a powerful post-training technique, enabling models to learn from feedback and align with human values. RL in MLLMs can be broadly categorized into two paradigms: (1) RL from human/AI

feedback (RLHF) [31, 50, 57, 63, 70, 74–76, 85, 88, 89, 92, 99, 102] and (2) RL with verifiable reward mechanisms [32, 37, 38, 64, 72, 93]. RLHF involves learning reward models from preference data before RL optimization, whereas the latter directly optimizes models using task-specific reward functions, bypassing explicit preference modeling. For example, DPO [55] is a notable implementation of RLHF and has been adopted by Emu3 [75] and HermesFlow [85] to narrow the performance gap between understanding and generation. In contrast, GRPO [60] exemplifies the second paradigm, simplifying reward formulation via group-wise relative advantage estimation. Our work also falls into this paradigm but diverges from prior work such as SimpleAR [72], which utilizes GRPO with external CLIP reward for autoregressive visual generation, and R1-like MLLMs [22, 38, 64, 93] that focus on incentivizing reasoning capabilities. First, our work demonstrates the significant potential of RL in co-optimizing understanding and generation, thereby broadening its applicability beyond reasoning. Moreover, we identify *semantic consistency rewards* and a *co-evolutionary reinforcement strategy* as crucial components in enhancing ULMs.

3 Methodology

3.1 Preliminary

Group relative policy optimization (GRPO) [60] is a value-free policy optimization algorithm with improved training stability and sample efficiency. Building upon PPO [58], GRPO introduces a group-wise relative advantage approach to bound policy updates while maintaining optimization flexibility. Let π_θ denote a policy parameterized by θ . Formally, given an input content c , the algorithm first samples a group of G outputs $\{o_1, o_2, \dots, o_G\}$ from the current policy $\pi_{\theta_{\text{old}}}$. Each output is then evaluated using predefined, verifiable reward functions, yielding the reward set $\{r_1, r_2, \dots, r_G\}$. These rewards are subsequently normalized to compute group-relative advantages as follows:

$$A_i = \frac{r_i - \text{mean}(\{r_1, r_2, \dots, r_G\})}{\text{std}(\{r_1, r_2, \dots, r_G\})}. \quad (1)$$

After obtaining the advantage set $\{A_1, A_2, \dots, A_G\}$ via group relative advantage estimation, the policy π_θ is optimized by maximizing the following objective:

$$\mathcal{L}(\theta) = \mathbb{E}_{\{o_i\}_{i=1}^G \sim \pi_{\theta_{\text{old}}}} \frac{1}{G} \sum_{i=1}^G \left[\frac{\pi_\theta(o_i)}{\pi_{\theta_{\text{old}}}(o_i)} A_i - \beta \mathbb{D}_{\text{KL}}(\pi_\theta \parallel \pi_{\text{ref}}) \right], \quad (2)$$

where \mathbb{D}_{KL} denotes the KL-divergence used to constrain the deviation between π_θ and its reference policy π_{ref} , and β is a regularization coefficient.

3.2 Pilot Exploration

Given the exceptional performance and data efficiency of DeepSeek-R1-Zero [18], we explore the potential of ULMs to enhance understanding and generation capabilities without dependence on task-specific supervised fine-tuning. To accomplish this, we curate a dataset¹ comprising 16K samples sourced from the COCO 2017 train split [35]. Each sample includes a real image, an associated caption as a textual prompt for visual generation, and a corresponding QA pair for the multimodal understanding task. We adopt CLIP Score [54] as the verifiable reward for image generation, and a combination of formatting correctness and answer accuracy as the reward for text generation. We investigate four distinct RL paradigms: (i) *separate RL*, where understanding and generation tasks are independently optimized under their respective reward mechanisms; (ii) *separate RL followed by weight merging*, where each

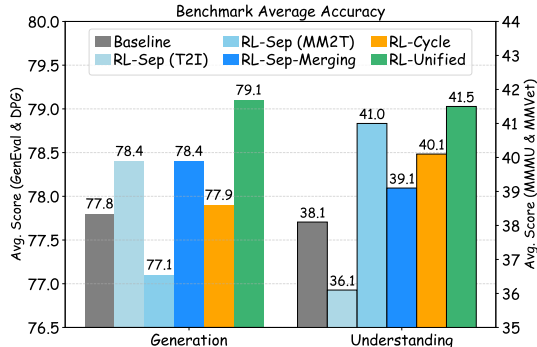


Figure 1: **Results of different RL paradigms.** Janus-Pro-1B [7] serves as the baseline.

under their respective reward mechanisms; (ii) *separate RL followed by weight merging*, where each

¹https://huggingface.co/datasets/mm-vl/x2x_rft_16k

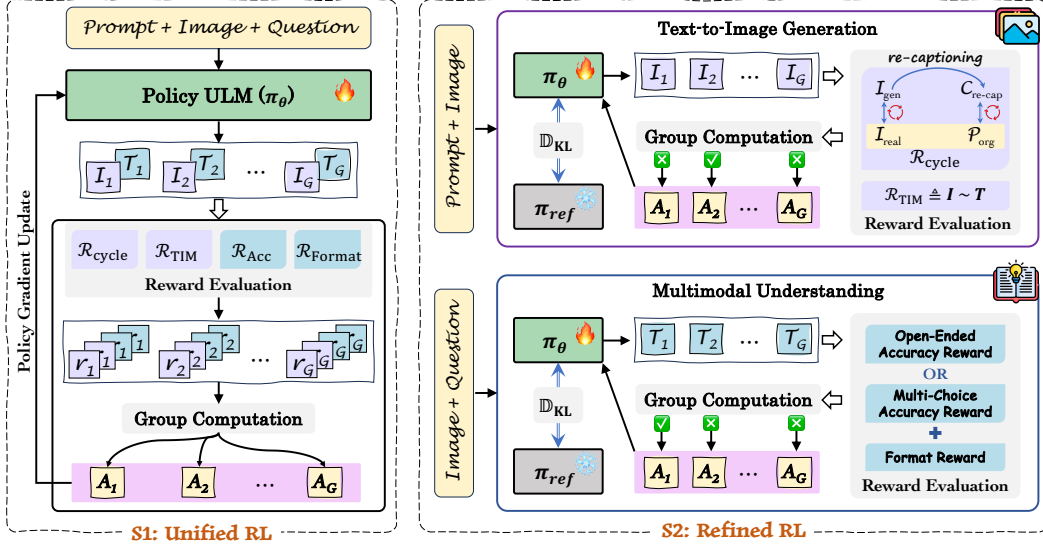


Figure 2: **Overview of CoRL**, a co-evolutionary reinforcement learning framework to jointly improve the dual capabilities of ULMs. CoRL adopts a two-stage RL procedure, comprising a unified RL stage for joint optimization and a refined RL stage for task-specific enhancement.

task is separately optimized, and the resulting weights are subsequently merged using a Gaussian distribution-based merging strategy [61] to incorporate both abilities; (iii) *cycle RL*, which applies a scheduled alternation between the two tasks throughout the training process; and (iv) *unified RL*, in which both tasks are jointly optimized within a unified paradigm to promote co-evolution.

As presented in Figure 1, we observe that (1) direct task-specific RL fails to achieve the expected improvements for ULMs, particularly in the visual generation task, and may even impair performance on the other task; and (2) unified RL demonstrates substantial advantages over alternative paradigms. These findings indicate that the dual capabilities co-evolving within a shared training framework contribute to more effective cross-task synergy and knowledge transfer.

3.3 Co-Reinforcement Learning

3.3.1 Verifiable Reward for Multimodal modeling

In this section, we develop a suite of verifiable rewards for multimodal modeling, which provide clear and objective feedback to steer ULMs toward generating high-quality image and text outputs.

Bidirectional Cycle Consistency Reward in Text-to-Image Generation. To encourage ULMs to generate images that faithfully reflect the concepts and entities described in the input prompt, we introduce a bidirectional cycle consistency reward $\mathcal{R}_{\text{cycle}}$, which measures the consistency between predictions and ground truth in both visual and textual spaces. For visual consistency, we adopt LPIPS [97] to assess the patch-level perceptual similarity between the real image $\mathcal{I}_{\text{real}}$ and the synthesized image \mathcal{I}_{gen} . Textual consistency is implemented in a re-captioning manner. Specifically, we first employ BLIP [29] to generate a caption $\mathcal{C}_{\text{re-cap}}$ for each synthesized image, and then compute the SPICE [1] score between $\mathcal{C}_{\text{re-cap}}$ and its original prompt \mathcal{P}_{org} to measure semantic fidelity. The combined bidirectional cycle reward is defined as:

$$\mathcal{R}_{\text{cycle}} = 1 - \text{LPIPS}(\mathcal{I}_{\text{real}}, \mathcal{I}_{\text{gen}}) + \text{SPICE}(\mathcal{P}_{\text{org}}, \mathcal{C}_{\text{re-cap}}). \quad (3)$$

This bidirectional reward forms a closed feedback loop that promotes mutual consistency between text and image, effectively penalizing hallucinated content and reinforcing prompt-adherent visual generation by simultaneously optimizing for both visual and textual consistency.

Text-Image Matching Reward. While CLIP Score [54] provides a holistic measure of text-image alignment, it underperforms in Sec. 3.2 due to its limited ability to assess fine-grained semantics. To address this limitation, we instead propose a text-image matching reward \mathcal{R}_{TIM} , which leverages the ULM itself to assess cross-modal alignment at the token level. Given a textual representation $\mathbf{T} = \{t_1, t_2, \dots, t_{L_t}\} \in \mathbb{R}^{L_t \times d}$ of the prompt and the corresponding visual representation $\mathbf{I} =$

$\{\mathbf{i}_1, \mathbf{i}_2, \dots, \mathbf{i}_{L_i}\} \in \mathbb{R}^{L_i \times d}$ of a generated image, the reward is computed as:

$$\mathcal{R}_{\text{TIM}} = \frac{1}{2} \left(\frac{1}{L_i} \sum_{j=1}^{L_i} \max_{k \in [1, L_t]} \cos(\mathbf{i}_j, \mathbf{t}_k) + \frac{1}{L_t} \sum_{k=1}^{L_t} \max_{j \in [1, L_i]} \cos(\mathbf{t}_k, \mathbf{i}_j) \right), \quad (4)$$

where L_t and L_i are the lengths of textual and visual token sequences, and d is the embedding dimension. This reward captures the fine-grained correspondence between textual concepts and visual elements through maximum cosine similarity, ensuring that each visual token aligns with its most relevant textual counterpart and vice versa.

Accuracy Reward in Multimodal Question Answering. Accuracy rewards leverage task-specific metrics to directly evaluate the correctness of ULM predictions. We consider two accuracy rewards tailored to different question types: $\mathcal{R}_{\text{MCQ-Acc}}$ for multi-choice questions and $\mathcal{R}_{\text{OE-Acc}}$ for open-ended questions. These rewards follow a binary evaluation mechanism, assigning a value of 1 when the predicted answer matches the ground truth and 0 otherwise.

Format Reward in Text Generation. To encourage ULMs to generate structured and interpretable textual responses, we adopt the format reward [18], which requires the model to enclose its thinking process inside `<think> ... </think>`, and provide its final answer within `<answer>` and `<answer>` tags. The format reward $\mathcal{R}_{\text{Format}}$ returns 1 for strict compliance, and 0 otherwise.

3.3.2 Unified Reinforcement Learning for Synergistic Multimodal Modeling

As illustrated in Figure 2, the policy ULM first undergoes unified reinforcement learning with diverse rewards across understanding and generation tasks. This unified process aims to jointly enhance its dual capabilities and establish a solid foundation for subsequent task-specific refinement.

Reward Function and Training Objective. To ensure diversity and complementarity in reward signals for unified multimodal modeling, we formulate a joint reward function as

$$\mathcal{R}_{\text{Uni-S1}} = \mathcal{R}_{\text{cycle}} + \mathcal{R}_{\text{TIM}} + \lambda \cdot (\mathcal{R}_{\text{Acc}} + \mathcal{R}_{\text{Format}}), \quad (5)$$

where λ is a coefficient that balances the two types of rewards. During training, given an input prompt and an image-question pair, the policy model $\pi_{\theta_{\text{old}}}$ first generates G candidate responses, $o = \{(\mathcal{I}_1, \mathcal{T}_1), (\mathcal{I}_2, \mathcal{T}_2), \dots, (\mathcal{I}_G, \mathcal{T}_G)\}$, each comprising a synthesized image \mathcal{I} and a CoT-format solution \mathcal{T} . Concurrently, the joint reward function $\mathcal{R}_{\text{Uni-S1}}$ evaluates each candidate pair, yielding the reward set $r = \{r_1, r_2, \dots, r_G\}$. These rewards are subsequently normalized according to Eq. (1) to compute the corresponding group-relative advantages $A = \{A_1, A_2, \dots, A_G\}$. The new policy model π_{θ} is then updated by maximizing the following GRPO-based objective:

$$\mathcal{L}_{\text{S1}} = \mathbb{E}_{\{o_i\}_{i=1}^G \sim \pi_{\theta_{\text{old}}}} \frac{1}{G} \sum_{i=1}^G \frac{\pi_{\theta}(o_i)}{\pi_{\theta_{\text{old}}}(o_i)} A_i, \text{ where } o_i = (\mathcal{I}_i, \mathcal{T}_i). \quad (6)$$

Notably, based on empirical findings from recent work [87], we omit the KL-divergence constraint during this stage to improve both optimization efficiency and generalization capability.

Training Data. To support unified RL for synergistic multimodal modeling, we curate a comprehensive dataset comprising 22K samples², which follows the data structure established in Sec. 3.2. Each sample includes a *real image*, a *prompt* for visual generation, and a *CoT-format QA pair* for multimodal understanding. This balanced data composition facilitates joint optimization of dual capabilities within a unified framework, while preserving the granularity of task-specific supervision.

3.3.3 Refined Reinforcement Learning for Task-specific Enhancement

After completing unified RL, as shown in Figure 2, we apply a targeted learning strategy to further enhance the task-specific performance of the policy model. This second-stage optimization leverages task-specific rewards and tailored datasets for individual tasks.

Reward Function and Training Objective. For text-to-image generation, the reward is defined as $\mathcal{R}_{\text{T2I-S2}} = \mathcal{R}_{\text{cycle}} + \mathcal{R}_{\text{TIM}}$. For multimodal understanding, we define two distinct reward formulations: (1) $\mathcal{R}_{\text{MCQ-S2}} = \mathcal{R}_{\text{MCQ-Acc}} + \mathcal{R}_{\text{Format}}$ for multiple-choice questions, and (2) $\mathcal{R}_{\text{OE-S2}} = \mathcal{R}_{\text{OE-Acc}} + \mathcal{R}_{\text{Format}}$

²https://huggingface.co/datasets/mm-vl/x2x_rft_22k

Table 1: **Results on text-to-image generation benchmarks.** 🍀 and 🍃 denote models trained using DPO and GRPO strategies. The best performance in each category is highlighted in **bold**.

Model	Scale	Res.	Type	GenEval \uparrow				WISE \uparrow	DPG \uparrow	
				Two Obj.	Counting	Position	Color Attri.	Overall	Overall	Overall
\blacktriangledown <i>Generation Only</i>										
PixArt- α [4]	0.6B	512 ²	Diff	0.50	0.44	0.08	0.07	0.48	0.47	71.11
SDv1.5 [56]	0.9B	512 ²	Diff	0.38	0.35	0.04	0.06	0.43	0.32	63.18
SDv2.1 [56]	0.9B	512 ²	Diff	0.51	0.44	0.07	0.17	0.50	0.32	68.09
SD3-Medium [14]	2B	512 ²	Diff	0.94	0.72	0.33	0.60	0.74	0.42	84.08
SDXL [51]	2.6B	1024 ²	Diff	0.74	0.39	0.15	0.23	0.55	0.43	74.65
DALL-E 3 [3]	-	1024 ²	Diff	0.87	0.47	0.43	0.45	0.67	-	83.50
LlamaGen [62]	0.8B	256 ²	F-AR	0.34	0.21	0.07	0.04	0.32	-	65.16
SimpleAR [72] 🍃	1.5B	1024 ²	F-AR	0.90	-	0.28	0.45	0.63	-	81.97
\blacktriangledown <i>Unified Understanding and Generation</i>										
TokenFlow [53]	8B	256 ²	F-AR	0.60	0.41	0.16	0.24	0.55	-	73.38
Emu3 [75]	8B	512 ²	F-AR	-	-	-	-	0.66	0.39	80.60
Emu3-DPO [75] 🍀	8B	512 ²	F-AR	-	-	-	-	0.64	-	81.60
LWM [36]	7B	512 ²	F-AR	0.41	0.46	0.09	0.15	0.47	-	-
Orthus [26]	7B	512 ²	AR-Diff	-	-	-	-	0.58	0.27	-
Janus-Pro [7]	7B	384 ²	F-AR	0.89	0.59	0.79	0.88	0.80	0.35	84.19
ILLUME+ [21]	3B	384 ²	AR-Diff	0.88	0.62	0.42	0.53	0.72	-	-
D-DiT [34]	2B	512 ²	Diff	0.80	0.54	0.32	0.50	0.65	-	-
Harmon [80]	1.5B	512 ²	F-AR	0.86	0.66	0.74	0.48	0.76	0.41	-
show-o [83]	1.3B	512 ²	AR-Diff	0.80	0.66	0.31	0.50	0.68	0.35	67.48
HermesFlow [85] 🍀	1.3B	512 ²	AR-Diff	0.84	0.66	0.32	0.52	0.69	-	70.22
Janus [78]	1.3B	384 ²	F-AR	0.68	0.30	0.46	0.42	0.61	0.23	79.68
Janus-Pro [7]	1.5B	384 ²	F-AR	0.82	0.51	0.65	0.56	0.73	0.26	82.63
ULM-R1 🍃	1.5B	384 ²	F-AR	0.85	0.71	0.68	0.80	0.77	0.33	83.92

for open-ended questions. The training objective in this stage adheres to the standard GRPO formulation in Eq. (2), with the appropriate task-specific reward (\mathcal{R}_{T2I-S2} , \mathcal{R}_{MCQ-S2} , or \mathcal{R}_{OE-S2}) replacing A_i depending on the task. To ensure stable optimization, we reintroduce the KL-divergence constraint at this stage to limit policy deviation from the reference distribution.

Training Data. For text-to-image generation, we continue training on the curated dataset introduced in Sec. 3.2. For multimodal understanding, we utilize two specialized datasets: `mcot_r1_mcq`³ for multiple-choice questions and `mcot_r1_vqa`⁴ for open-ended questions. These task-specific datasets enable the model to develop more refined and robust capabilities within each task domain.

4 Experiment

4.1 Experimental Setups

Evaluation Benchmarks. We evaluate visual generation capabilities on the GenEval [17], WISE [46], and DPG-Bench [20] benchmarks. GenEval employs an object-centric evaluation protocol to assess compositional and attribute-level alignment, while DPG-Bench adopts a VQA-based setting to evaluate dense prompt-following and semantic fidelity. WISE provides a holistic evaluation of models’ world knowledge, considering consistency, realism, and aesthetics. We also evaluate multimodal understanding capabilities across diverse benchmarks. Specifically, MMStar [5], MMMU [91], and WeMath (Math^{We}) [52] are used for multi-choice evaluation, while MMVet [90], POPE [33], and LogicVista (Logic^{VT}) [82] are used for open-ended evaluation. In addition, we employ MathVista (Math^{VT}) [40], MathVerse-Vision (Math^{VS}) [95], and MathVision (Math^{Vis}) [73] to assess complex mathematical reasoning capabilities, covering both multi-choice and open-ended QA formats. On these benchmarks, we compute accuracy using the toolkit VLMEvalKit [12].

Implementation Details. We develop ULM-R1 using Janus-Pro-1B [7] as the baseline ULM for unified multimodal understanding and generation. To ensure reproducibility and scalability, our RL training is built upon the trl [68] framework. In the unified RL stage, we employ the AdamW

³https://huggingface.co/datasets/mm-vl/mcot_r1_mcq_66k

⁴https://huggingface.co/datasets/mm-vl/mcot_r1_vqa_66k

Table 2: **Results on multimodal understanding benchmarks.** The best performance within each category is highlighted in **bold**. † denotes results obtained from our evaluation.

Model	LLM	Multi-Choice (MC) †			Open-Ended (OE) †			MC&OE Mixed †		
		MMMU	MMStar	Math ^{We}	MMVet	POPE	Logic ^{VT}	Math ^{VT}	Math ^{VS}	Math ^{Vis}
▼ Understanding Only										
SmolVLM [45]	SmolLM2-1.7B	38.8	41.7	9.1	33.8	85.5	28.0	43.6	12.6	12.8
SAIL-VL [10]	Qwen2.5-1.5B	44.1	56.5	14.6	44.2	88.1	30.4	62.8	17.4	17.3
Ovis2 [42]	Qwen2.5-1.5B	45.6	56.7	9.9	58.3	87.8	34.7	64.1	29.4	17.7
InternVL3 [103]	Qwen2.5-1.5B	48.7	61.1	22.9	67.0	90.1	34.7	57.6	24.5	20.2
Qwen2.5-VL [2]	Qwen2.5-3B	51.2	56.3	22.9	60.0	85.9	40.3	61.2	31.2	21.9
LMM-R1 [49]	Qwen2.5-3B	-	58.0	-	-	-	-	63.2	41.6	26.4
▼ Unified Understanding and Generation										
ILLUME+ [21]	Qwen2.5-3B	44.3	-	-	40.3	87.6	-	-	-	-
Harmon [80]	Qwen2.5-1.5B	38.9	-	-	-	87.6	-	-	-	-
VILA-U [81]	LLaMA-2-7B	-	-	-	33.5	85.8	-	-	-	-
Orthus [26]	Chameleon-7B	28.2	-	-	-	79.6	-	-	-	-
UniToken [24]	Chameleon-7B	32.8	46.1	-	-	-	-	38.5	-	-
SGen-VL [28]	InternLM2-1.8B	34.2	-	-	34.5	85.3	-	42.7	-	-
Show-o [83]	Phi-1.3B	26.7	-	-	-	80.0	-	-	-	-
HermesFlow [85]	Phi-1.3B	28.3	-	-	-	81.4	-	-	-	-
Janus-Pro [7]	DeepSeek-LLM-7B	41.0	46.5	9.7	50.0	87.4	28.0	42.5	15.9	14.7
Janus [78]	DeepSeek-LLM-1.3B	30.5	37.6	3.4†	34.3	87.0	23.9†	33.7	14.9†	13.4†
Janus-Pro [7]	DeepSeek-LLM-1.5B	36.3	43.1†	5.9†	39.8	86.2	23.9†	37.3†	13.5†	13.4†
ULM-R1	DeepSeek-LLM-1.5B	42.3	47.6	21.1	43.9	88.9	34.5	42.5	25.4	22.0

optimizer with an initial learning rate of 4e-6 and a batch size of 16. We sample 8 responses for both understanding and generation tasks, and set the reward balancing factor in Eq. (5) to 0.8. In the refined RL stage, we sample 16 responses for both multimodal understanding and text-to-image generation tasks. Additionally, we reduce the learning rate to 1e-6 to facilitate fine-grained optimization. All training is conducted on 8 NVIDIA H20 (96G) GPUs. During inference, greedy decoding is used for text generation in multimodal understanding tasks. For text-to-image generation, we employ classifier-free guidance (CFG) [19] with a guidance weight set to 5. More details on the training data and settings are provided in App. A.

4.2 Quantitative Results

Text-to-Image Generation. Table 1 presents a comprehensive comparison between ULM-R1 and state-of-the-art models across three visual generation benchmarks. Among unified models, our model ranks second on both GenEval and WISE benchmarks. Notably, it achieves balanced performance across diverse task categories within GenEval, with the best score of 0.71 in object counting. When compared with specialized generation-only models, ULM-R1 surpasses the top performer SD3-Medium [14] by a slight margin (0.77 vs. 0.74 on GenEval). Moreover, ULM-R1 shows consistent improvements over its base model across all benchmarks. These results collectively demonstrate the effectiveness and advantage of our CoRL in enhancing visual generation quality.

Multimodal Understanding. Results are shown in Table 2. We continue to apply the Gaussian distribution-based merging strategy [61] to combine the two task-specific policy models for mixed QA format evaluation. Overall, ULM-R1 markedly outperforms existing unified models across most benchmarks, and substantially narrows the performance gap with leading understanding-only MLLMs of comparable model scale. More specifically, our model achieves state-of-the-art performance among unified models on MMStar (47.6), WeMath (21.1), LogicVista (34.5), and on several mixed-format math benchmarks, including MathVerse (25.4) and MathVision (22.0). Particularly, ULM-R1 demonstrates considerable improvements over its base model in mathematical and logical reasoning tasks, achieving gains of **15.2** on WeMath and **10.6** on LogicVista. These results not only demonstrate the effectiveness of CoRL in enhancing ULMs’ understanding capabilities, but also establish that reinforcement learning provides a data-efficient pathway for achieving both robust generalization and sophisticated reasoning capabilities, without the need for large-scale supervised data.

Table 3: **Comparison between different RL paradigms for ULMs.** The cold SFT data is consist of x2x_rft_22k, mcot_r1_mcq (22K), and mcot_r1_vqa (22K). #7: CoRL.

#	Ablated Setting	Stage	GenEval	DPG	MMMU	Math ^{We}	MMVet	Logic ^{VT}
0	Baseline	-	73.0	82.6	36.3	5.9	39.8	23.9
1	+ Cold-SFT	S1	72.8 (-0.3)	82.5 (-0.1)	41.0 (+4.7)	18.0 (+12.1)	42.0 (+2.2)	27.9 (+4.0)
2	+ Unified-RL	S1	75.9 (+2.9)	83.3 (+0.7)	40.3 (+4.0)	14.0 (+8.1)	42.5 (+2.7)	30.2 (+6.3)
3	+ Refined-RL (T2I)	S2	75.1 (+2.1)	83.0 (+0.4)	/	/	/	/
4	+ Refined-RL (MM2T-MC)	S2	/	/	39.6 (+3.3)	15.8 (+9.9)	/	/
5	+ Refined-RL (MM2T-OE)	S2	/	/	/	/	42.2 (+2.4)	29.5 (+5.6)
6	+ Refined-RL w/ Cold-SFT	S1&S2	74.5 (+1.5)	82.8 (+0.2)	41.8 (+5.5)	22.5 (+16.6)	43.7 (+3.9)	35.9 (+12.0)
7	+ Refined-RL w/ Unified-RL	S1&S2	77.3 (+4.3)	83.9 (+1.3)	42.3 (+6.0)	21.1 (+15.2)	43.9 (+4.1)	34.5 (+10.6)

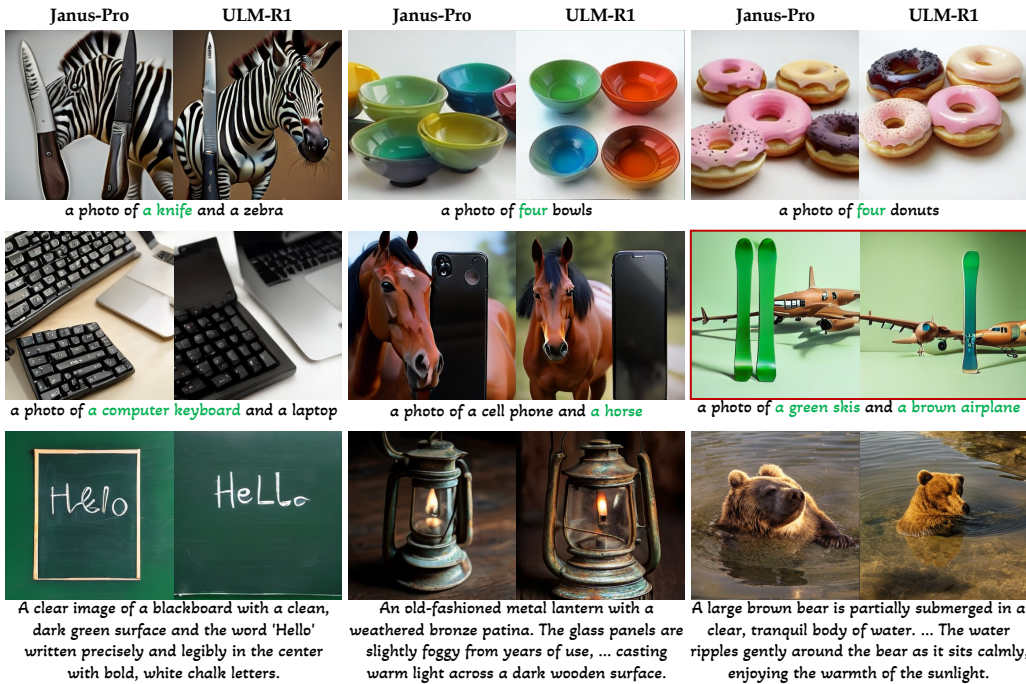


Figure 3: **Qualitative comparison of text-to-image generation** between Janus-Pro and ULM-R1. The red box marks an exemplary failure case.

4.3 Qualitative Results

In this section, we first present a qualitative comparison between ULM-R1 and Janus-Pro on visual generation, as illustrated in Figure 3. The results clearly showcase that ULM-R1 achieves superior text-to-image alignment and object grounding across diverse prompts, with especially notable improvements in spatial object arrangement and compositional consistency. Furthermore, as shown in Figure 4, we visualize several representative examples of multimodal understanding. Compared to Janus-Pro, ULM-R1 exhibits significantly enhanced understanding capabilities, particularly in mathematical reasoning. These comprehensive qualitative results demonstrate the effectiveness of CoRL in simultaneously improving both visual generation and multimodal understanding in ULMs.

4.4 Ablation Studies

In this section, we primarily validate the effectiveness of our training strategy and designed rewards.

Comparison Between Various RL Paradigms. As presented in Table 3, we conduct a comprehensive ablation study to evaluate the effects of different RL paradigms for ULMs. The results reveal two key findings: ▶ #2 vs. #1: Unified-RL effectively enhances both the generation and understanding capabilities of ULMs, whereas Cold-SFT has minimal impact on visual generation.

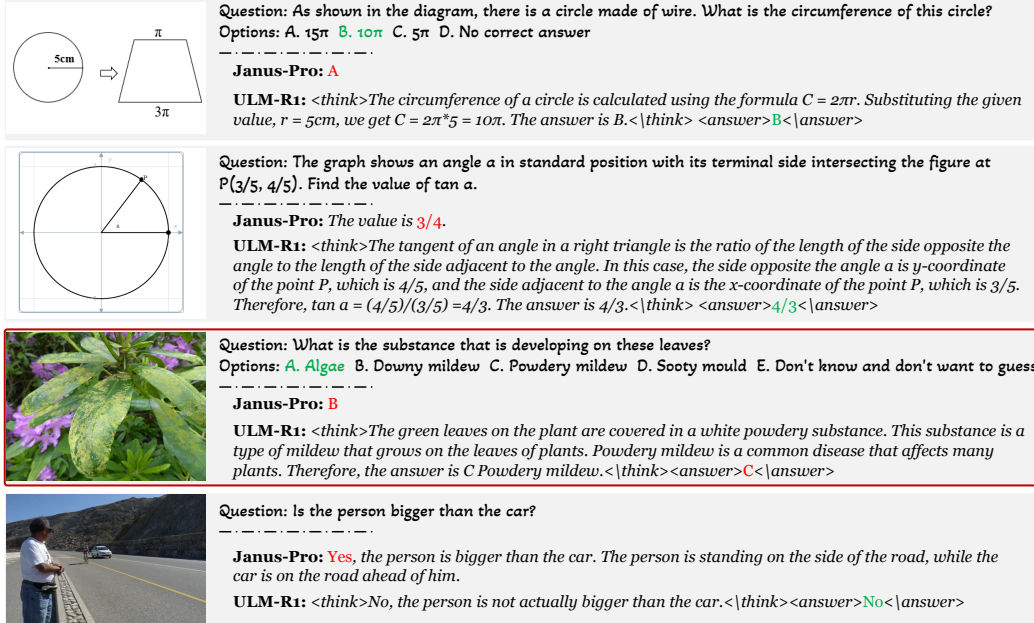


Figure 4: **Qualitative comparison of multimodal understanding** between Janus-Pro and ULM-R1. The red box marks an exemplary failure case.

► #7 vs. #6: Compared to the de facto paradigm, our CoRL consistently outperforms it on visual generation benchmarks while achieving comparable results on multimodal understanding benchmarks. These findings indicate that *unified RL provides a robust foundation for task-specific refinement, even without reliance on supervised data*. Additionally, CoRL consistently outperforms both its baseline and task-specific RL variants (#3-#5), achieving improvements of 2.1 points on GenEval (vs. generation-only RL, #3) and 5.3 points on WeMath (vs. understanding-only RL, #4). These results demonstrate the efficacy of CoRL as our final RL paradigm.

Rewards in Text-to-Image Generation. To assess the effectiveness of our proposed rewards for text-to-image generation, we conduct ablation experiments as detailed in Table 4. The results demonstrate that incorporating either reward individually improves performance over the baseline: $\mathcal{R}_{\text{cycle}}$ yields an increase of 2.1 in average score, while \mathcal{R}_{TIM} results in an increase of 0.8. Notably, combining both rewards leads to the best overall performance, achieving an average score of 80.6. These findings suggest a modest but complementary effect between $\mathcal{R}_{\text{cycle}}$ and \mathcal{R}_{TIM} , enhancing their joint benefit in enhancing visual generation quality.

Table 4: **Effect of visual generation rewards.**

#	$\mathcal{R}_{\text{cycle}}$	\mathcal{R}_{TIM}	GenEval	DPG	Avg. \uparrow
0			73.0	82.6	77.8
1	✓		76.2	83.5	79.9 (+2.1)
2		✓	74.1	83.0	78.6 (+0.8)
3	✓	✓	77.3	83.9	80.6 (+2.8)

5 Conclusion

In this work, we investigate how to jointly enhance the understanding and generation capabilities of ULMs, and propose a co-evolutionary RL framework (CoRL). Within the proposed CoRL, the policy model undergoes unified RL for joint optimization and refined RL for task-specific enhancement, yielding ULM-R1. Extensive evaluations across diverse understanding and generation benchmarks demonstrate the effectiveness of CoRL and the advantage of ULM-R1.

Limitation. Despite the substantial improvements achieved, several limitations remain that warrant further investigation. First, a notable performance gap still exists between generation and understanding tasks of ULMs. Second, our rewards for multimodal understanding are relatively simple and primary. These limitations highlight the need for more sophisticated RL designs that can further enhance understanding capabilities and narrow the performance gap. We hope our work provides valuable insights for future RL research in ULMs.

A Appendix

A.1 Training Data

Training Data for Unified Reinforcement Learning. To support synergistic multimodal modeling during unified RL, we curate a dataset (*i.e.*, `x2x_rft_22k`) that simultaneously involves text-to-image generation and multimodal understanding tasks. As illustrated in Figure 5, each sample includes a *real image*, a *prompt* for generation, and a *problem* for understanding. The real images are sourced from the COCO 2017 train split [35], while the problems and their corresponding solutions are adapted from A-OKVQA [59] and GPT-VQA [98]. In addition, prompts are selected from the original COCO captions based on their entity coverage with the problem solutions.

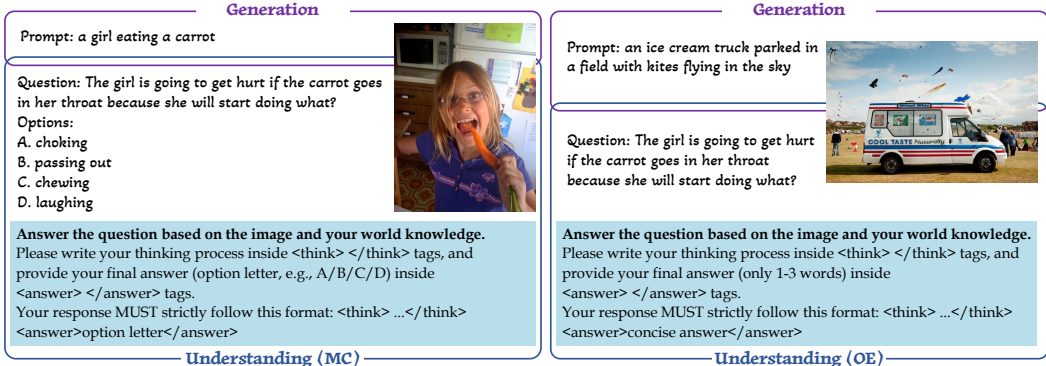


Figure 5: Illustration of training examples used in unified reinforcement learning.

Training Data for Refined Reinforcement Learning. In this stage, we collect three specialized datasets for task-specific RL. For text-to-image generation, we continue constructing a dataset (*i.e.*, `x2x_rft_16k`) with prompts derived from COCO captions. Moreover, we curate `mcot_r1_mcq` and `mcot_r1_vqa` for multiple-choice and open-ended multimodal understanding, respectively. These two datasets encompass a diverse range of multimodal tasks, including mathematical reasoning, science-problem solving, and visual commonsense reasoning, across multiple source datasets. Specifically, `mcot_r1_mcq` consists of A-OKVQA [59], M³CoT [6], SQA-IMG (train) [39], ArxivQA [30], TabMWP (MC) [41], and MAVIS-Instruct (MC) [96], while `mcot_r1_vqa` includes GeomVerse [25], R-CoT [9], TabMWP (OE) [41], and MAVIS-Instruct (OE) [96].

A.2 Supplementary Experimental Setups

Table 5 provides detailed hyperparameter settings for ULM-R1’s RL training.

Table 5: Training hyperparameter setting.

Configuration	Unified RL	Refined RL (T2I)	Refined RL (MM2T-MC)	Refined RL (MM2T-OE)
Number of sampled outputs (G)	8	16	16	16
Regularization coefficient of $\mathbb{D}_{\text{KL}}(\beta)$	0	0.02	0.02	0.02
Max prompt length	1024	256	1024	1024
Max completion length	512	/	512	512
Batch size	16	16	32	32
Peak learning rate	4e-6	1e-6	1e-6	1e-6
Epoch	1	1	1	1

References

- [1] Peter Anderson, Basura Fernando, Mark Johnson, and Stephen Gould. Spice: Semantic propositional image caption evaluation. In *ECCV*, pages 382–398, 2016. 4
- [2] Shuai Bai, Keqin Chen, Xuejing Liu, Jialin Wang, Wenbin Ge, Sibao Song, Kai Dang, Peng Wang, Shijie Wang, Jun Tang, et al. Qwen2. 5-vl technical report. *arXiv:2502.13923*, 2025. 7
- [3] James Betker, Gabriel Goh, Li Jing, Tim Brooks, Jianfeng Wang, Linjie Li, Long Ouyang, Juntang Zhuang, Joyce Lee, Yufei Guo, et al. Improving image generation with better captions, 2023. URL <https://cdn.openai.com/papers/dall-e-3.pdf>. 6
- [4] Junsong Chen, Jincheng Yu, Chongjian Ge, Lewei Yao, Enze Xie, Yue Wu, Zhongdao Wang, James Kwok, Ping Luo, Huchuan Lu, et al. Pixart-alpha: Fast training of diffusion transformer for photorealistic text-to-image synthesis. *arXiv:2310.00426*, 2023. 6
- [5] Lin Chen, Jinsong Li, Xiaoyi Dong, Pan Zhang, Yuhang Zang, Zehui Chen, Haodong Duan, Jiaqi Wang, Yu Qiao, Dahua Lin, et al. Are we on the right way for evaluating large vision-language models? *arXiv:2403.20330*, 2024. 6
- [6] Qiguang Chen, Libo Qin, Jin Zhang, Zhi Chen, Xiao Xu, and Wanxiang Che. M³CoT: A novel benchmark for multi-domain multi-step multi-modal chain-of-thought. *arXiv:2405.16473*, 2024. 10
- [7] Xiaokang Chen, Zhiyu Wu, Xingchao Liu, Zizheng Pan, Wen Liu, Zhenda Xie, Xingkai Yu, and Chong Ruan. Janus-pro: Unified multimodal understanding and generation with data and model scaling. *arXiv:2501.17811*, 2025. 1, 2, 3, 6, 7
- [8] Huilin Deng, Ding Zou, Rui Ma, Hongchen Luo, Yang Cao, and Yu Kang. Boosting the generalization and reasoning of vision language models with curriculum reinforcement learning. *arXiv:2503.07065*, 2025. 1
- [9] Linger Deng, Yuliang Liu, Bohan Li, Dongliang Luo, Liang Wu, Chengquan Zhang, Pengyuan Lyu, Ziyang Zhang, Gang Zhang, Errui Ding, et al. R-cot: Reverse chain-of-thought problem generation for geometric reasoning in large multimodal models. *arXiv:2410.17885*, 2024. 10
- [10] Hongyuan Dong, Zijian Kang, Weijie Yin, Xiao Liang, Chao Feng, and Jiao Ran. Scalable vision language model training via high quality data curation. *arXiv:2501.05952*, 2025. 7
- [11] Runpei Dong, Chunrui Han, Yuang Peng, Zekun Qi, Zheng Ge, Jinrong Yang, Liang Zhao, Jianjian Sun, Hongyu Zhou, Haoran Wei, et al. Dreamllm: Synergistic multimodal comprehension and creation. In *ICLR*, 2024. 2
- [12] Haodong Duan, Junming Yang, Yuxuan Qiao, Xinyu Fang, Lin Chen, Yuan Liu, Xiaoyi Dong, Yuhang Zang, Pan Zhang, Jiaqi Wang, et al. Vlmevalkit: An open-source toolkit for evaluating large multi-modality models. *arXiv:2407.11691*, 2024. 6
- [13] Patrick Esser, Robin Rombach, and Bjorn Ommer. Taming transformers for high-resolution image synthesis. In *CVPR*, pages 12873–12883, 2021. 2
- [14] Patrick Esser, Sumith Kulal, Andreas Blattmann, Rahim Entezari, Jonas Müller, Harry Saini, Yam Levi, Dominik Lorenz, Axel Sauer, Frederic Boesel, et al. Scaling rectified flow transformers for high-resolution image synthesis. In *ICML*, 2024. 6, 7
- [15] Lijie Fan, Luming Tang, Siyang Qin, Tianhong Li, Xuan Yang, Siyuan Qiao, Andreas Steiner, Chen Sun, Yuanzhen Li, Tao Zhu, et al. Unified autoregressive visual generation and understanding with continuous tokens. *arXiv:2503.13436*, 2025. 2
- [16] Yuying Ge, Sijie Zhao, Jinguo Zhu, Yixiao Ge, Kun Yi, Lin Song, Chen Li, Xiaohan Ding, and Ying Shan. Seed-x: Multimodal models with unified multi-granularity comprehension and generation. *arXiv:2404.14396*, 2024. 2
- [17] Dhruva Ghosh, Hannaneh Hajishirzi, and Ludwig Schmidt. Geneval: An object-focused framework for evaluating text-to-image alignment. In *NeurIPS*, pages 52132–52152, 2023. 6
- [18] Daya Guo, Dejian Yang, Haowei Zhang, Junxiao Song, Ruoyu Zhang, Runxin Xu, Qihao Zhu, Shirong Ma, Peiyi Wang, Xiao Bi, et al. Deepseek-r1: Incentivizing reasoning capability in llms via reinforcement learning. *arXiv:2501.12948*, 2025. 1, 3, 5
- [19] Jonathan Ho and Tim Salimans. Classifier-free diffusion guidance. *arXiv:2207.12598*, 2022. 7

- [20] Xiwei Hu, Rui Wang, Yixiao Fang, Bin Fu, Pei Cheng, and Gang Yu. Ella: Equip diffusion models with llm for enhanced semantic alignment. *arXiv:2403.05135*, 2024. 6
- [21] Runhui Huang, Chunwei Wang, Junwei Yang, Guansong Lu, Yunlong Yuan, Jianhua Han, Lu Hou, Wei Zhang, Lanqing Hong, Hengshuang Zhao, et al. Illume+: Illuminating unified mllm with dual visual tokenization and diffusion refinement. *arXiv:2504.01934*, 2025. 2, 6, 7
- [22] Wenxuan Huang, Bohan Jia, Zijie Zhai, Shaosheng Cao, Zheyu Ye, Fei Zhao, Zhe Xu, Yao Hu, and Shaohui Lin. Vision-r1: Incentivizing reasoning capability in multimodal large language models. *arXiv:2503.06749*, 2025. 1, 3
- [23] Dongzhi Jiang, Ziyu Guo, Renrui Zhang, Zhuofan Zong, Hao Li, Le Zhuo, Shilin Yan, Pheng-Ann Heng, and Hongsheng Li. T2i-r1: Reinforcing image generation with collaborative semantic-level and token-level cot. *arXiv:2505.00703*, 2025. 1
- [24] Yang Jiao, Haibo Qiu, Zequn Jie, Shaoxiang Chen, Jingjing Chen, Lin Ma, and Yu-Gang Jiang. Unitoken: Harmonizing multimodal understanding and generation through unified visual encoding. *arXiv:2504.04423*, 2025. 7
- [25] Mehran Kazemi, Hamidreza Alvani, Ankit Anand, Jialin Wu, Xi Chen, and Radu Soricut. Geomverse: A systematic evaluation of large models for geometric reasoning. *arXiv:2312.12241*, 2023. 10
- [26] Siqi Kou, Jiachun Jin, Chang Liu, Ye Ma, Jian Jia, Quan Chen, Peng Jiang, and Zhijie Deng. Orthus: Autoregressive interleaved image-text generation with modality-specific heads. *arXiv:2412.00127*, 2024. 2, 6, 7
- [27] Komal Kumar, Tajamul Ashraf, Omkar Thawakar, Rao Muhammad Anwer, Hisham Cholakkal, Mubarak Shah, Ming-Hsuan Yang, Phillip HS Torr, Fahad Shahbaz Khan, and Salman Khan. Llm post-training: A deep dive into reasoning large language models. *arXiv:2502.21321*, 2025. 1
- [28] Hao Li, Changyao Tian, Jie Shao, Xizhou Zhu, Zhaokai Wang, Jinguo Zhu, Wenhan Dou, Xiaogang Wang, Hongsheng Li, Lewei Lu, et al. Synergen-vl: Towards synergistic image understanding and generation with vision experts and token folding. *arXiv:2412.09604*, 2024. 2, 7
- [29] Junnan Li, Dongxu Li, Silvio Savarese, and Steven Hoi. Blip-2: Bootstrapping language-image pre-training with frozen image encoders and large language models. In *ICML*, pages 19730–19742, 2023. 4
- [30] Lei Li, Yuqi Wang, Runxin Xu, Peiyi Wang, Xiachong Feng, Lingpeng Kong, and Qi Liu. Multimodal arxiv: A dataset for improving scientific comprehension of large vision-language models. *arXiv:2403.00231*, 2024. 10
- [31] Lei Li, Zhihui Xie, Mukai Li, Shunian Chen, Peiyi Wang, Liang Chen, Yazheng Yang, Benyou Wang, Lingpeng Kong, and Qi Liu. Vfeedback: A large-scale ai feedback dataset for large vision-language models alignment. *arXiv:2410.09421*, 2024. 3
- [32] Xinhao Li, Ziang Yan, Desen Meng, Lu Dong, Xiangyu Zeng, Yinan He, Yali Wang, Yu Qiao, Yi Wang, and Limin Wang. Videochat-r1: Enhancing spatio-temporal perception via reinforcement fine-tuning. *arXiv:2504.06958*, 2025. 3
- [33] Yifan Li, Yifan Du, Kun Zhou, Jinpeng Wang, Wayne Xin Zhao, and Ji-Rong Wen. Evaluating object hallucination in large vision-language models. *arXiv:2305.10355*, 2023. 6
- [34] Zijie Li, Henry Li, Yichun Shi, Amir Barati Farimani, Yuval Kluger, Linjie Yang, and Peng Wang. Dual diffusion for unified image generation and understanding. *arXiv:2501.00289*, 2024. 6
- [35] Tsung-Yi Lin, Michael Maire, Serge Belongie, James Hays, Pietro Perona, Deva Ramanan, Piotr Dollár, and C Lawrence Zitnick. Microsoft coco: Common objects in context. In *ECCV*, pages 740–755, 2014. 3, 10
- [36] Hao Liu, Wilson Yan, Matei Zaharia, and Pieter Abbeel. World model on million-length video and language with ringattention. In *ICLR*, 2025. 1, 2, 6
- [37] Yuqi Liu, Bohao Peng, Zhisheng Zhong, Zihao Yue, Fanbin Lu, Bei Yu, and Jiaya Jia. Seg-zero: Reasoning-chain guided segmentation via cognitive reinforcement. *arXiv:2503.06520*, 2025. 1, 3
- [38] Ziyu Liu, Zeyi Sun, Yuhang Zang, Xiaoyi Dong, Yuhang Cao, Haodong Duan, Dahua Lin, and Jiaqi Wang. Visual-rft: Visual reinforcement fine-tuning. *arXiv:2503.01785*, 2025. 1, 3

- [39] Pan Lu, Swaroop Mishra, Tanglin Xia, Liang Qiu, Kai-Wei Chang, Song-Chun Zhu, Oyvind Tafjord, Peter Clark, and Ashwin Kalyan. Learn to explain: Multimodal reasoning via thought chains for science question answering. In *NeurIPS*, pages 2507–2521, 2022. 10
- [40] Pan Lu, Hritik Bansal, Tony Xia, Jiacheng Liu, Chunyuan Li, Hannaneh Hajishirzi, Hao Cheng, Kai-Wei Chang, Michel Galley, and Jianfeng Gao. Mathvista: Evaluating mathematical reasoning of foundation models in visual contexts. *arXiv:2310.02255*, 2023. 6
- [41] Pan Lu, Liang Qiu, Kai-Wei Chang, Ying Nian Wu, Song-Chun Zhu, Tanmay Rajpurohit, Peter Clark, and Ashwin Kalyan. Dynamic prompt learning via policy gradient for semi-structured mathematical reasoning. In *ICLR*, 2023. 10
- [42] Shiyin Lu, Yang Li, Qing-Guo Chen, Zhao Xu, Weihua Luo, Kaifu Zhang, and Han-Jia Ye. Ovis: Structural embedding alignment for multimodal large language model. *arXiv:2405.20797*, 2024. 7
- [43] Chuofan Ma, Yi Jiang, Junfeng Wu, Jihan Yang, Xin Yu, Zehuan Yuan, Bingyue Peng, and Xiaojuan Qi. Unitok: A unified tokenizer for visual generation and understanding. *arXiv:2502.20321*, 2025. 2
- [44] Yiyang Ma, Xingchao Liu, Xiaokang Chen, Wen Liu, Chengyue Wu, Zhiyu Wu, Zizheng Pan, Zhenda Xie, Haowei Zhang, Liang Zhao, et al. Janusflow: Harmonizing autoregression and rectified flow for unified multimodal understanding and generation. *arXiv:2411.07975*, 2024. 2
- [45] Andrés Marafioti, Orr Zohar, Miquel Farré, Merve Noyan, Elie Bakouch, Pedro Cuenca, Cyril Zakka, Loubna Ben Allal, Anton Lozhkov, Nouamane Tazi, et al. Smolvlm: Redefining small and efficient multimodal models. *arXiv:2504.05299*, 2025. 7
- [46] Yuwei Niu, Munan Ning, Mengren Zheng, Bin Lin, Peng Jin, Jiaqi Liao, Kunpeng Ning, Bin Zhu, and Li Yuan. Wise: A world knowledge-informed semantic evaluation for text-to-image generation. *arXiv:2503.07265*, 2025. 6
- [47] OpenAI. Openai o1 system card. *arXiv:2412.16720*, 2024. 1
- [48] OpenAI. Openai o3 and o4-mini system card, 2025. URL <https://cdn.openai.com/pdf/2221c875-02dc-4789-800b-e7758f3722c1/o3-and-o4-mini-system-card.pdf>. 1
- [49] Yingzhe Peng, Gongrui Zhang, Miaosen Zhang, Zhiyuan You, Jie Liu, Qipeng Zhu, Kai Yang, Xingzhong Xu, Xin Geng, and Xu Yang. Lmm-r1: Empowering 3b llms with strong reasoning abilities through two-stage rule-based rl. *arXiv:2503.07536*, 2025. 1, 7
- [50] Renjie Pi, Tianyang Han, Wei Xiong, Jipeng Zhang, Runtao Liu, Rui Pan, and Tong Zhang. Strengthening multimodal large language model with bootstrapped preference optimization. In *ECCV*, pages 382–398, 2024. 3
- [51] Dustin Podell, Zion English, Kyle Lacey, Andreas Blattmann, Tim Dockhorn, Jonas Müller, Joe Penna, and Robin Rombach. Sdxl: Improving latent diffusion models for high-resolution image synthesis. *arXiv:2307.01952*, 2023. 6
- [52] Runqi Qiao, Qiuna Tan, Guanting Dong, Minhui Wu, Chong Sun, Xiaoshuai Song, Zhuoma GongQue, Shanglin Lei, Zhe Wei, Miaoxuan Zhang, et al. We-math: Does your large multimodal model achieve human-like mathematical reasoning? *arXiv:2407.01284*, 2024. 6
- [53] Liao Qu, Huichao Zhang, Yiheng Liu, Xu Wang, Yi Jiang, Yiming Gao, Hu Ye, Daniel K Du, Zehuan Yuan, and Xinglong Wu. Tokenflow: Unified image tokenizer for multimodal understanding and generation. *arXiv:2412.03069*, 2024. 2, 6
- [54] Alec Radford, Jong Wook Kim, Chris Hallacy, Aditya Ramesh, Gabriel Goh, Sandhini Agarwal, Girish Sastry, Amanda Askell, Pamela Mishkin, Jack Clark, et al. Learning transferable visual models from natural language supervision. In *ICML*, pages 8748–8763, 2021. 3, 4
- [55] Rafael Rafailov, Archit Sharma, Eric Mitchell, Christopher D Manning, Stefano Ermon, and Chelsea Finn. Direct preference optimization: Your language model is secretly a reward model. In *NeurIPS*, pages 53728–53741, 2023. 1, 3
- [56] Robin Rombach, Andreas Blattmann, Dominik Lorenz, Patrick Esser, and Björn Ommer. High-resolution image synthesis with latent diffusion models. In *CVPR*, pages 10684–10695, 2022. 6
- [57] Pritam Sarkar, Sayna Ebrahimi, Ali Etemad, Ahmad Beirami, Sercan Ö Arık, and Tomas Pfister. Mitigating object hallucination via data augmented contrastive tuning. *arXiv:2405.18654*, 2024. 3

- [58] John Schulman, Filip Wolski, Prafulla Dhariwal, Alec Radford, and Oleg Klimov. Proximal policy optimization algorithms. *arXiv:1707.06347*, 2017. 3
- [59] Dustin Schwenk, Apoorv Khandelwal, Christopher Clark, Kenneth Marino, and Roozbeh Mottaghi. A-OKVQA: A benchmark for visual question answering using world knowledge. In *ECCV*, pages 146–162, 2022. 10
- [60] Zhihong Shao, Peiyi Wang, Qihao Zhu, Runxin Xu, Junxiao Song, Xiao Bi, Haowei Zhang, Mingchuan Zhang, YK Li, Y Wu, et al. Deepseekmath: Pushing the limits of mathematical reasoning in open language models. *arXiv:2402.03300*, 2024. 1, 3
- [61] Chongjie Si, Jingjing Jiang, and Wei Shen. Unveiling the mystery of weight in large foundation models: Gaussian distribution never fades. *arXiv:2501.10661*, 2025. 4, 7
- [62] Peize Sun, Yi Jiang, Shoufa Chen, Shilong Zhang, Bingyue Peng, Ping Luo, and Zehuan Yuan. Autoregressive model beats diffusion: Llama for scalable image generation. *arXiv:2406.06525*, 2024. 2, 6
- [63] Zhiqing Sun, Sheng Shen, Shengcao Cao, Haotian Liu, Chunyuan Li, Yikang Shen, Chuang Gan, Liang-Yan Gui, Yu-Xiong Wang, Yiming Yang, et al. Aligning large multimodal models with factually augmented rlhf. *arXiv:2309.14525*, 2023. 3
- [64] Huajie Tan, Yuheng Ji, Xiaoshuai Hao, Minglan Lin, Pengwei Wang, Zhongyuan Wang, and Shanghang Zhang. Reason-rlft: Reinforcement fine-tuning for visual reasoning. *arXiv:2503.20752*, 2025. 1, 3
- [65] Chameleon Team. Chameleon: Mixed-modal early-fusion foundation models. *arXiv:2405.09818*, 2024. 2
- [66] Kimi Team, Angang Du, Bofei Gao, Bowei Xing, Changjiu Jiang, Cheng Chen, Cheng Li, Chenjun Xiao, Chenzhuang Du, Chonghua Liao, et al. Kimi k1. 5: Scaling reinforcement learning with llms. *arXiv:2501.12599*, 2025. 1
- [67] Guiyao Tie, Zeli Zhao, Dingjie Song, Fuyang Wei, Rong Zhou, Yurou Dai, Wen Yin, Zhejian Yang, Jiangyue Yan, Yao Su, et al. A survey on post-training of large language models. *arXiv:2503.06072*, 2025. 1
- [68] Leandro von Werra, Younes Belkada, Lewis Tunstall, Edward Beeching, Tristan Thrush, Nathan Lambert, Shengyi Huang, Kashif Rasul, and Quentin Gallouédec. Trl: Transformer reinforcement learning. <https://github.com/huggingface/trl>, 2020. 6
- [69] Chunwei Wang, Guansong Lu, Junwei Yang, Runhui Huang, Jianhua Han, Lu Hou, Wei Zhang, and Hang Xu. Illume: Illuminating your llms to see, draw, and self-enhance. *arXiv:2412.06673*, 2024. 2
- [70] Fei Wang, Wenxuan Zhou, James Y Huang, Nan Xu, Sheng Zhang, Hoifung Poon, and Muhao Chen. mdpo: Conditional preference optimization for multimodal large language models. *arXiv:2406.11839*, 2024. 1, 3
- [71] Jane X Wang, Zeb Kurth-Nelson, Dhruva Tirumala, Hubert Soyer, Joel Z Leibo, Remi Munos, Charles Blundell, Dharshan Kumaran, and Matt Botvinick. Learning to reinforcement learn. *arXiv:1611.05763*, 2016. 2
- [72] Junke Wang, Zhi Tian, Xun Wang, Xinyu Zhang, Weilin Huang, Zuxuan Wu, and Yu-Gang Jiang. Simplear: Pushing the frontier of autoregressive visual generation through pretraining, sft, and rl. *arXiv:2504.11455*, 2025. 1, 3, 6
- [73] Ke Wang, Junting Pan, Weikang Shi, Zimu Lu, Mingjie Zhan, and Hongsheng Li. Measuring multimodal mathematical reasoning with math-vision dataset. *arXiv:2402.14804*, 2024. 6
- [74] Weiyun Wang, Zhe Chen, Wenhai Wang, Yue Cao, Yangzhou Liu, Zhangwei Gao, Jinguo Zhu, Xizhou Zhu, Lewei Lu, Yu Qiao, et al. Enhancing the reasoning ability of multimodal large language models via mixed preference optimization. *arXiv:2411.10442*, 2024. 3
- [75] Xinlong Wang, Xiaosong Zhang, Zhengxiong Luo, Quan Sun, Yufeng Cui, Jinsheng Wang, Fan Zhang, Yueze Wang, Zhen Li, Qiyang Yu, et al. Emu3: Next-token prediction is all you need. *arXiv:2409.18869*, 2024. 2, 3, 6
- [76] Yibin Wang, Yuhang Zang, Hao Li, Cheng Jin, and Jiaqi Wang. Unified reward model for multimodal understanding and generation. *arXiv:2503.05236*, 2025. 1, 3

- [77] Marco A Wiering and Martijn Van Otterlo. Reinforcement learning. *Adaptation, learning, and optimization*, 12(3):729, 2012. 2
- [78] Chengyue Wu, Xiaokang Chen, Zhiyu Wu, Yiyang Ma, Xingchao Liu, Zizheng Pan, Wen Liu, Zhenda Xie, Xingkai Yu, Chong Ruan, et al. Janus: Decoupling visual encoding for unified multimodal understanding and generation. *arXiv:2410.13848*, 2024. 2, 6, 7
- [79] Junfeng Wu, Yi Jiang, Chuofan Ma, Yuliang Liu, Hengshuang Zhao, Zehuan Yuan, Song Bai, and Xiang Bai. Liquid: Language models are scalable multi-modal generators. *arXiv:2412.04332*, 2024. 2
- [80] Size Wu, Wenwei Zhang, Lumin Xu, Sheng Jin, Zhonghua Wu, Qingyi Tao, Wentao Liu, Wei Li, and Chen Change Loy. Harmonizing visual representations for unified multimodal understanding and generation. *arXiv:2503.21979*, 2025. 6, 7
- [81] Yecheng Wu, Zhuoyang Zhang, Junyu Chen, Haotian Tang, Dacheng Li, Yunhao Fang, Ligeng Zhu, Enze Xie, Hongxu Yin, Li Yi, et al. Vila-u: a unified foundation model integrating visual understanding and generation. In *ICLR*, 2025. 1, 2, 7
- [82] Yijia Xiao, Edward Sun, Tianyu Liu, and Wei Wang. Logicvista: Multimodal llm logical reasoning benchmark in visual contexts. *arXiv:2407.04973*, 2024. 6
- [83] Jinheng Xie, Weijia Mao, Zechen Bai, David Junhao Zhang, Weihao Wang, Kevin Qinghong Lin, Yuchao Gu, Zhijie Chen, Zhenheng Yang, and Mike Zheng Shou. Show-o: One single transformer to unify multimodal understanding and generation. In *ICLR*, 2025. 1, 2, 6, 7
- [84] Rongchang Xie, Chen Du, Ping Song, and Chang Liu. Muse-vl: Modeling unified vlm through semantic discrete encoding. *arXiv:2411.17762*, 2024. 2
- [85] Ling Yang, Xinchen Zhang, Ye Tian, Chenming Shang, Minghao Xu, Wentao Zhang, and Bin Cui. Hermesflow: Seamlessly closing the gap in multimodal understanding and generation. *arXiv:2502.12148*, 2025. 2, 3, 6, 7
- [86] Jiahui Yu, Xin Li, Jing Yu Koh, Han Zhang, Ruoming Pang, James Qin, Alexander Ku, Yuanzhong Xu, Jason Baldridge, and Yonghui Wu. Vector-quantized image modeling with improved vqgan. *arXiv:2110.04627*, 2021. 2
- [87] Qiyang Yu, Zheng Zhang, Ruofei Zhu, Yufeng Yuan, Xiaochen Zuo, Yu Yue, Tiantian Fan, Gaohong Liu, Lingjun Liu, Xin Liu, et al. Dapo: An open-source llm reinforcement learning system at scale. *arXiv:2503.14476*, 2025. 5
- [88] Tianyu Yu, Yuan Yao, Haoye Zhang, Taiwen He, Yifeng Han, Ganqu Cui, Jinyi Hu, Zhiyuan Liu, Hai-Tao Zheng, Maosong Sun, et al. Rlhf-v: Towards trustworthy mllms via behavior alignment from fine-grained correctional human feedback. In *CVPR*, pages 13807–13816, 2024. 1, 3
- [89] Tianyu Yu, Haoye Zhang, Yuan Yao, Yunkai Dang, Da Chen, Xiaoman Lu, Ganqu Cui, Taiwen He, Zhiyuan Liu, Tat-Seng Chua, et al. Rlaif-v: Aligning mllms through open-source ai feedback for super gpt-4v trustworthiness. *arXiv:2405.17220*, 2024. 3
- [90] Weihao Yu, Zhengyuan Yang, Linjie Li, Jianfeng Wang, Kevin Lin, Zicheng Liu, Xinchao Wang, and Lijuan Wang. Mm-vet: Evaluating large multimodal models for integrated capabilities. *arXiv:2308.02490*, 2023. 6
- [91] Xiang Yue, Yuansheng Ni, Kai Zhang, Tianyu Zheng, Ruoqi Liu, Ge Zhang, Samuel Stevens, Dongfu Jiang, Weiming Ren, Yuxuan Sun, Cong Wei, Botao Yu, Ruibin Yuan, Renliang Sun, Ming Yin, Boyuan Zheng, Zhenzhu Yang, Yibo Liu, Wenhao Huang, Huan Sun, Yu Su, and Wenhui Chen. Mmmu: A massive multi-discipline multimodal understanding and reasoning benchmark for expert agi. In *CVPR*, pages 9556–9567, 2024. 6
- [92] Simon Zhai, Hao Bai, Zipeng Lin, Jiayi Pan, Peter Tong, Yifei Zhou, Alane Suhr, Saining Xie, Yann LeCun, Yi Ma, et al. Fine-tuning large vision-language models as decision-making agents via reinforcement learning. In *NeurIPS*, pages 110935–110971, 2024. 3
- [93] Yufei Zhan, Yousong Zhu, Shurong Zheng, Hongyin Zhao, Fan Yang, Ming Tang, and Jinqiao Wang. Vision-rl: Evolving human-free alignment in large vision-language models via vision-guided reinforcement learning. *arXiv:2503.18013*, 2025. 1, 3
- [94] Jingyi Zhang, Jiaying Huang, Huanjin Yao, Shunyu Liu, Xikun Zhang, Shijian Lu, and Dacheng Tao. R1-vl: Learning to reason with multimodal large language models via step-wise group relative policy optimization. *arXiv:2503.12937*, 2025. 1

- [95] Renrui Zhang, Dongzhi Jiang, Yichi Zhang, Haokun Lin, Ziyu Guo, Pengshuo Qiu, Aojun Zhou, Pan Lu, Kai-Wei Chang, Peng Gao, et al. Mathverse: Does your multi-modal llm truly see the diagrams in visual math problems? *arXiv:2403.14624*, 2024. [6](#)
- [96] Renrui Zhang, Xinyu Wei, Dongzhi Jiang, Yichi Zhang, Ziyu Guo, Chengzhuo Tong, Jiaming Liu, Aojun Zhou, Bin Wei, Shanghang Zhang, et al. Mavis: Mathematical visual instruction tuning. *arXiv:2407.08739*, 2024. [10](#)
- [97] Richard Zhang, Phillip Isola, Alexei A Efros, Eli Shechtman, and Oliver Wang. The unreasonable effectiveness of deep features as a perceptual metric. In *CVPR*, pages 586–595, 2018. [4](#)
- [98] Zhiyuan Zhao, Linke Ouyang, Bin Wang, Siyuan Huang, Pan Zhang, Xiaoyi Dong, Jiaqi Wang, and Conghui He. Mllm-dataengine: An iterative refinement approach for mllm. *arXiv:2308.13566*, 2023. [10](#)
- [99] Zhiyuan Zhao, Bin Wang, Linke Ouyang, Xiaoyi Dong, Jiaqi Wang, and Conghui He. Beyond hallucinations: Enhancing lvlms through hallucination-aware direct preference optimization. *arXiv:2311.16839*, 2023. [3](#)
- [100] Chunting Zhou, Lili Yu, Arun Babu, Kushal Tirumala, Michihiro Yasunaga, Leonid Shamis, Jacob Kahn, Xuezhe Ma, Luke Zettlemoyer, and Omer Levy. Transfusion: Predict the next token and diffuse images with one multi-modal model. *arXiv:2408.11039*, 2024. [2](#)
- [101] Guanghao Zhou, Panjia Qiu, Cen Chen, Jie Wang, Zheming Yang, Jian Xu, and Minghui Qiu. Reinforced mllm: A survey on rl-based reasoning in multimodal large language models. *arXiv:2504.21277*, 2025. [1](#), [2](#)
- [102] Yiyang Zhou, Chenhang Cui, Rafael Rafailov, Chelsea Finn, and Huaxiu Yao. Aligning modalities in vision large language models via preference fine-tuning. *arXiv:2402.11411*, 2024. [3](#)
- [103] Jinguo Zhu, Weiyun Wang, Zhe Chen, Zhaoyang Liu, Shenglong Ye, Lixin Gu, Yuchen Duan, Hao Tian, Weijie Su, Jie Shao, et al. Internvl3: Exploring advanced training and test-time recipes for open-source multimodal models. *arXiv:2504.10479*, 2025. [7](#)